Thermodynamic properties of Ar, Kr and Xe from a Monte Carlo-based perturbation theory with an effective two-body Lennard-Jones potential

B.P. Akhouri [a], J.R. Solana [b],*

[a] Department of Physics. Suraj Singh Memorial College, Ranchi, 834008, Jharkhand, India
[b] Department of Applied Physics. University of Cantabria, Avda. de los Castros s/n, Santander, 39005, Spain

ARTICLE INFO

ABSTRACT

A third-order perturbation theory is used to obtain the equilibrium properties of Ar, Kr and Xe over wide ranges of temperatures and densities. The theory belongs to the framework of the inverse temperature expansion of the Helmholtz free energy, with the perturbation terms determined from Monte Carlo simulation. The interactions are modeled by an effective two-body Lennard-Jones potential incorporating the main contribution of the three-body interactions. To this end, the ratio of three-body to two-body configuration energies have been determined also from Monte Carlo simulation. The results for the pressure and energy at supercritical temperatures are in quite good agreement with experimental data. The liquid–vapor coexistence is also reproduced fairly well, although for Ar and Kr the critical temperature is slightly overestimated as well as the liquid densities at low temperatures, and the coexistence densities of Xe are slightly overestimated for the vapor and underestimated for the liquid near the critical point. In any case, the calculations show a remarkable improvement in the predicted coexistence curve with including the three-body contribution.

1. Introduction

The thermodynamic properties of simple model fluids can be obtained from integral equation theory (IET), from a combination of perturbation theory with integral equation theory (IEPT), or from conventional perturbation theory (PT) like the Barker–Henderson (BH) and related theories, as well as from computer simulation.[1] However, IET and IEPT theories generally are nonanalytical and computationally demanding, which is undesirable for practical applications, and PTs based on the high temperature expansion (HTE) of the Helmholtz free energy generally provide accurate results only for the first-order perturbation term, which may be insufficient at low temperatures where higher-order terms may play a nonnegligible role.

Alternatively, a number of the lower order perturbation terms in the HTE can be obtained from computer simulation, using the procedure devised by Barker and Henderson [2,3]. This procedure is less computationally demanding and once the perturbation terms are obtained, the thermodynamic properties can be obtained for wide ranges of temperatures en densities with little computational effort. This is the approach used in this work for the heavy noble gases Ar, Kr and Xe.

---

* Corresponding author.
  E-mail address: solanajr@unican.es (J.R. Solana).

[1] See Ref. [1] for a review on IET, IEPT, PT, and related theories for several potential models.

Simple two-body potential models are useful in the development of theories for the thermodynamic properties of fluids and solids. However, when going from model to real fluids, even in the case of a simple fluid such as argon, the contribution of three-body interactions cannot be neglected. Directly incorporating three-body interactions in theoretical models is unfeasible and in computer simulations is computationally very demanding.

Averaged three-body interactions can be separately calculated either from approximate theories or from computer simulation and then their contribution to the thermodynamic properties added to those from the two-body interactions. Within the framework of perturbation theories a number of approximations along this line have been proposed. Thus, Barker et al. [4] developed a perturbation theory for Ar based on the second-order perturbation theory for two-body interactions modeled by the Barker–Pompe potential with an additional perturbation term to approximately account for the three-body interactions, with the latter determined from both theory and simulation and conveniently parametrized as a function of the density for practical applications. Another approximation of this kind has been very recently developed by Dridi et al. [5] for noble gases. In this case, a perturbation theory based on the first-order mean spherical approximation (FMSA) for the hard-core two Yukawa potential [6] was used for the two-body interactions together with the Barker et al. [4] parametrization for the contribution of the three-body interactions. It is to be noted that the latter was developed for the Barker–Bobetic potential for Ar and, therefore, there is not reason to think that it will be accurate for other dense noble gases.

A different way of taking into account the effect of the three-body interactions in the thermodynamic properties consists in using effective two-body potentials that include the three-body contribution. To this end, del Río et al. [7–10] introduced a family of effective potentials, denoted as approximate non conformal (ANC) potentials, involving a number of parameters that are determined from the condition that certain thermodynamic properties, such as the second and third virial coefficients and the pressure at some selected states, determined from the effective potential, for example by computer simulation, fit the corresponding experimental data. The effective potential obtained in this way is state-dependent.

The Axilrod–Teller [11] approximation gives accurate account of the main contribution to the three-body interactions. Stenschke [12], by averaging the Axilrod–Teller interaction, found that the result is of the form of a two-body potential that can be incorporated to the true two-body potential giving rise to an effective two-body potential linearly dependent on density. In a similar way, a simple density-dependent expression relating the three-body and two-body interactions, thus allowing to merge both kind of interactions into an effective two-body potential, has been developed by Sadus et al. [13–16], on the basis of computer simulations for Ar, Kr and Xe in the liquid phase at subcritical temperatures considering pairwise interactions as given by the BFW potential [17] plus three-body interactions.

However, the conclusions of the above-cited papers are limited to the BFW potential and to the relatively limited temperature and density ranges considered. Here we are interested in analyzing the relation between three-body (3B) and two-body (2B) contributions to the configurational energy of the heavy noble gases for much wider temperature and density ranges, covering a great part of the fluid phase for which there are available experimental data for the thermodynamic properties. In addition, we are interested in checking whether a similar relationship holds also for the Lennard-Jones potential, which has the advantage over the BFW potential that can be expressed exclusively in terms of reduced units, thus potentially allowing to develop a single 2B effective potential that includes the 3B interactions applicable to the three noble gases Ar, Kr and Xe.

The aim of this work is to test the performance of a perturbation theory with and effective two-body Lennard-Jones potential to obtain the liquid–vapor coexistence densities as well as the pressure and energy at supercritical temperatures for the heavy noble gases. To this end, first we have carried out computer simulations to obtain the 2B and 3B contributions, E_2 and E_3 respectively, to the configurational energy over wide ranges of temperature and density for the BFW and LJ potentials for Ar. These potentials are presented in the next section in which also are described the simulations performed, the ratios E_3/E_2 for both potential models are analyzed and, in the case of the LJ potential at supercritical temperatures, fitted to a temperature- and density-dependent expression suitable to incorporate the three-body interactions into an effective two-body LJ potential. Section 3 gives a short account about the Monte Carlo-based perturbation theory (MCPT) used in this work and the simulations performed to obtain the first three perturbation terms in the expansion. The results for the thermodynamic properties of Ar, Kr and Xe are compared in Section 4 with the NIST experimental data and the concluding remarks are presented in the last section.

2. Two-body and three-body potentials for argon

2.1. Two-body potential models for argon

An accurate potential model for the heavy noble gases is the Barker–Fisher–Watts potential [17]

$$u_{\mathrm{BFW}}(x) = \varepsilon_{\mathrm{BFW}} \left\{ \left[A_0 + A_1(x-1) + A_2(x-1)^2 + A_3(x-1)^3 + A_4(x-1)^4 \right. \right.$$

$$\left. \left. + A_5(x-1)^5 \right] \times \mathrm{Exp}\left[\alpha(x-1) \right] - \left(\frac{C_6}{\delta + x^6} + \frac{C_8}{\delta + x^8} + \frac{C_{10}}{\delta + x^{10}} \right) \right\}, \tag{1}$$

Table 1
Parameters in the BFW potential (1) for Ar from Ref. [17].

$\varepsilon_{\mathrm{BFW}}/k\,(\mathrm{K})$	$\sigma_{\mathrm{BFW}}\,(\text{Å})$	$r_m\,(\text{Å})$	α	δ	
142.095	3.3605	3.7612	12.5	0.01	
A_0	A_1	A_2	A_3	A_4	A_5
0.27783	−4.50431	−8.331215	−25.2696	−102.0195	−113.25
C_6	C_8	C_{10}			
1.10727	0.1697	0.013611			

Table 2
Lennard-Jones potential parameters and nonadditive coefficients for Ar, Kr and Xe.

$\sigma_{\mathrm{LJ}}\,(\text{Å})$	$\varepsilon_{\mathrm{LJ}}/k\,(\mathrm{K})$	Source	$\nu \times 10^{108}\,\mathrm{J}\,m^9$ [21]
		Argon	
3.403	119.7	This work[a]	7.35
3.403	119.5	Ref. [20].[b]	
3.408–3.42	119.49–120.32	[22,23].[c]	
		Krypton	
3.64	168.7	This work[a]	22.30
3.64	164.4	Ref. [20].[b]	
3.591–3.68	166.67–175.34	Refs. [22–24].[c]	
		Xenon	
4.07	223.6	This work[a]	79.05
3.96	231.1	Ref. [20].[b]	
4.06–4.08	224.5–226.51	Refs. [22,23,25].[c]	

[a]From second virial coefficient data.
[b]From the lattice constant and sublimation energy of the solid.
[c]Range of values in the literature.

with $x = r/r_m$, where r_m is the position of the minimum of the potential. The parameters of the BFW potential for Ar are listed in Table 1.

However, here we are mainly focused on the Lennard-Jones potential model

$$u_{\mathrm{LJ}}(r) = 4\varepsilon_{\mathrm{LJ}}\left[\left(\frac{\sigma_{\mathrm{LJ}}}{r}\right)^{12} - \left(\frac{\sigma_{\mathrm{LJ}}}{r}\right)^{6}\right], \tag{2}$$

also frequently used for noble gases. The choice of the parameters σ_{LJ} and $\varepsilon_{\mathrm{LJ}}$ is of crucial importance because they have a strong influence on the accuracy of the calculated thermodynamic properties. These parameters can be obtained from experimental equilibrium or transport properties. As we are concerned here with equilibrium properties, we must resort to the parameters determined from some of them. This is done most frequently from second virial coefficient data. The problem is that the values of the parameters determined in this way reported in the literature spam over considerable ranges, especially for Kr and Xe. Therefore, we have started with determining these parameters from the smoothed data recommended in Ref. [18]. To this end, we have fitted the data to the series expansion of the second virial coefficient for the LJ fluid [19]. We have considered only the second virial coefficient data for supercritical temperatures, because at lower temperatures they are subjected to considerable experimental errors. The results are listed in Table 2, where we have included also for reference the values determined from solid state properties [20] and the ranges of the parameter values, determined from measured second virial coefficients, collected from the literature in a non-exhaustive search. It is to be noted that for Ar the values of σ_{LJ} and $\varepsilon_{\mathrm{LJ}}$ determined here are nearly equal to those determined from solid state properties [20], for Kr the values of σ_{LJ} are also equal and those of $\varepsilon_{\mathrm{LJ}}$ are close to each other, whereas for Xe the differences between the two sources for the parameters are remarkable.

As seen in Fig. 1-(a) both potentials for Ar are quite similar in shape. The resemblance is still greater if we adopt for the LJ potential the same value of ε as for the BFW potential, as seen in Fig. 1-(b). A similar situation arises for Kr and Xe.

2.2. Three-body interactions

There are different contributions to the three-body dispersion interactions, arising from combinations of multipole moments [26]. The leading contribution is that from the triple–dipole interactions which are accurately given by the Axilrod–Teller (AT) [11] expression

$$u_{ijk} = \nu\,\frac{(1 + 3\cos\theta_i \cos\theta_j \cos\theta_k)}{(r_{ij}r_{ik}r_{jk})^3}, \tag{3}$$
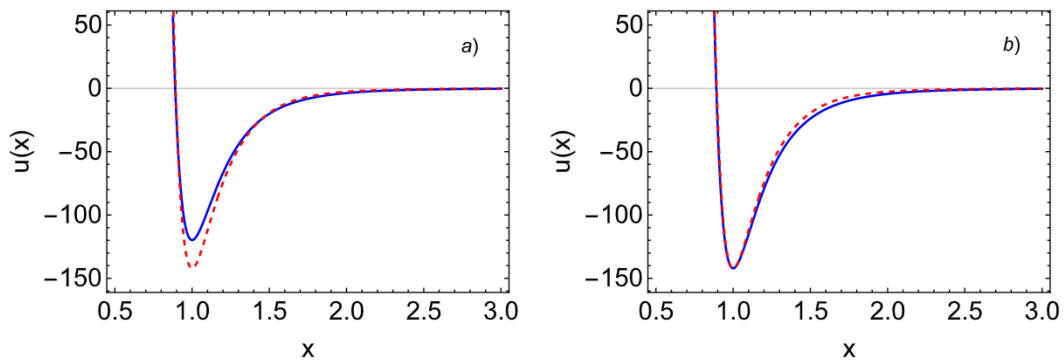
Fig. 1. Lennard-Jones potential (solid curves) compared with the BFW potential (dashed curves) for Ar, (a) with $\varepsilon_{LJ}/k = 119.7$, (b) with $\varepsilon_{LJ}/k = 142.095$.

where ν is the nonadditive coefficient for argon. Other third-order multipole interactions largely cancel out with fourth-order triple–dipole interactions [27], so that only the AT contribution to the three-body dispersion interactions needs to be considered as a good approximation.

Marcelli and Sadus [13,15] performed computer simulations to obtain the relative contribution of two-body (E_2) and three-body (E_3) interactions to the configurational energy of argon, krypton and xenon in the liquid phase with the BFW potential for the 2B interactions and the AT approximation for the 3B interactions. They considered a temperature range covering the coexistence region[2] and density ranges covering the liquid phase near coexisence.[3] They found a simple relationship for all these fluids, namely

$$\frac{E_3}{E_2} = \lambda \frac{\nu \rho}{\varepsilon \sigma^6}, \tag{4}$$

where $\rho = N/V$ is the number density and $\lambda = -2/3$. Later, Wang and Sadus [16] from new computer simulations for $T^* \sim 1$ and $0.4 \le \rho^* \le -0.8$, with $\rho^* = \rho\sigma^3$, found $\lambda = -0.85$. These authors, advised against the use of that relationship with an effective potential like that of Lennard-Jones. However, as we have seen in Fig. 1 both, the LJ and BFW potentials, have a quite similar shape for argon, and so it is expected that the ratio E_3/E_2 will behave in a similar way for the two potentials. Similar considerations apply to Kr and Xe. In any case, considering larger temperature and density ranges, including liquid and gas phases, it seems likely that such a simple relationship will no longer be valid. This question will be analyzed in the next section.

2.3. Monte Carlo simulations for the two-body and three-body contributions to the configurational energy of argon

In order to check whether the simple relationship (4) between three-body and two-body contributions to the configurational energy holds also for the Lennard-Jones fluid, we have performed *NVT* Monte Carlo simulations for both, the BFW and LJ potentials for argon. We used a system consisting in $N = 864$ particles initially placed in an FCC configuration within a box with volume $V = L^3$ with periodic boundary conditions. The systems was equilibrated for $N_e = 2 \times 10^4$ cycles, each of them consisting in N attempted particle moves, after which the contributions E_2 and E_3 were measured for the next $N_c = 5 \times 10^4$ cycles. In the calculation of E_2 the cut off distance of the potential was settled to $r_c^* = 3.0$, where $r^* = r/\sigma$, and the usual correction for the truncation of the potential was applied. In the calculation of E_3 the cut off distance was settled to $L/4$ because for larger distances the three-body interactions are negligible [27]. First, we considered a temperature $T = 140$ K, which is equivalent to a reduced temperature $T^* = 1.17$ for the LJ potential and to $T^* = 0.985$ for the BFW potential, and a reduced density range $0.5 \le \rho^* \le 0.7$, belonging to the liquid region. The results are plotted in Fig. 2. We can see that the roughly constant value for λ in Eq. (4), as reported by Sadus et al. [13,15,16] for the liquid phase at subcritical temperatures is supported by our results. From our simulations we obtain $\lambda = -0.77$ for LJ and $\lambda = -0.88$ for BFW.

However, when we consider also supercritical temperatures and a wider range of densities, the situation is quite different, as shown in Fig. 3. From the figure, it is clear that the above-mentioned ratio is both temperature and density dependent.

---

[2] For argon the experimental coexistence temperatures lie in the range $0.6 \lesssim T^* \lesssim 1$, with $T^* = kT/\varepsilon$ for the BFW value of ε quoted in Table 1.
[3] Roughly $0.4 \lesssim \rho^* \lesssim 0.8$ for the BFW value of σ quoted in Table 1.
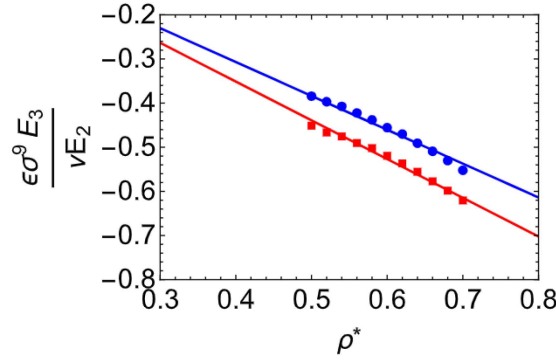
Fig. 2. Ratio of the three-body to two-body energies for argon at $T = 140\,$K with the LJ (circles) and BFW (squares) potentials as a function of the reduced density ρ^*. The solid lines are linear fittings.
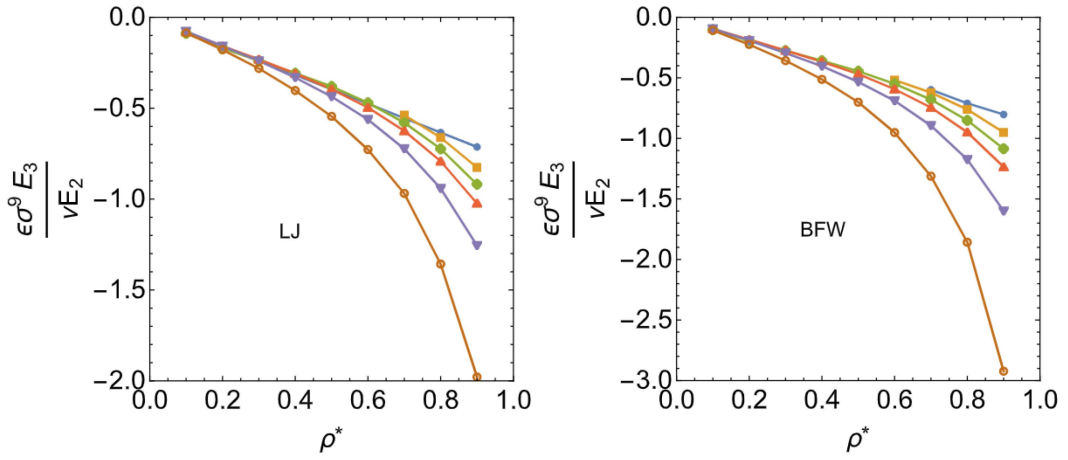

Fig. 3. Ratio of the three-body to two-body energies for argon with the LJ (left) and BFW (right) potentials as a function of the reduced density ρ^* for different reduced temperatures $T^* = 0.7, 1.0, 1.5, 2.0, 3.0,$ and 5.0, respectively, from top down. (Note that the reduced temperatures and densities are not equivalent for both potentials because the values of ε and σ are different). The curves are guides for the eye.

2.4. Effective temperature- and density-dependent potential for argon including the contribution of three-body interactions

We have fitted the simulation data analyzed in the previous section of the ratio

$$\frac{\varepsilon\sigma^9 E_3}{\nu\rho^* E_2} = \lambda \tag{5}$$

for the LJ potential to a function of the reduced density and temperature in the form

$$\lambda(\rho^*, T^*) = \sum_{i=1}^{4} \sum_{j=0}^{4} a_{ij} \frac{\rho^{*i}}{T^{*j}}. \tag{6}$$

The corresponding parameters a_{ij} are listed in Table 3.

Following Marcelli et al. [15], this will allow us to include the three-body interactions into an effective two-body potential of the form

$$u_{\text{eff}}(r) = u_2(r)\left[1 + \frac{\nu}{\varepsilon\sigma^9}\lambda(\rho^*, T^*)\right], \tag{7}$$

where $u_2(r)$ accounts for the two-body LJ potential.

Table 3
Parameters a_{ij} in eq. (6) for the LJ potential.

i	j				
	0	1	2	3	4
1	−0.231135	−1.363491	0.332008	1.522619	−0.570183
2	−10.339254	52.489802	−95.522035	77.252201	−22.792761
3	25.007885	−134.069029	261.136087	−217.350307	64.170784
4	−21.304910	112.411477	−220.968616	183.328674	−53.498016

3. Monte Carlo-based perturbation theory for the effective two-body Lennard-Jones fluid

3.1. The reference system

In perturbation theory for fluids with spherically-symmetric interactions, the potential is considered as the sum of two contributions: a reference potential $u_0(r)$, and a perturbation $u_1(r)$. Usually the reference potential accounts for the repulsive forces and is approximated by a hard-sphere (HS) potential. Therefore, for soft-core potentials, as is the LJ one, a suitable criterion must be used to determine and effective HS diameter. To this end, several prescriptions have been proposed in the literature. We will focus here on the Weeks–Chandler–Andersen (WCA) [28,29] and Lado [30] approximations. In the WCA perturbation theory, the reference and perturbation potentials are defined by

$$u_0(r) = \begin{cases} u(r) + \varepsilon, & r < r_m \\ 0, & r > r_m \end{cases}, \tag{8}$$

and

$$u_1(r) = \begin{cases} -\varepsilon, & r < r_m \\ u(r), & r > r_m \end{cases}, \tag{9}$$

respectively, where $r_m = 2^{1/6}\sigma$ is the position of the minimum of the LJ potential. In addition, the reference fluid with potential $u_0(r)$ is approximated by a fluid of hard spheres with diameter determined from the condition

$$\int_0^\infty y_{HS}(r; d_{WCA})\Delta e(r; d_{WCA})r^2 dr = 0, \tag{10}$$

where

$$\Delta e(r; d_{WCA}) = e^{-\beta u_0(r)} - e^{-\beta u_{HS}(r; d_{WCA})} \tag{11}$$

is the so-called "blip function",

$$y_{HS}(r; d_{WCA}) = g_{HS}(r)e^{\beta u_{HS}(r; d_{WCA})} \tag{12}$$

is the background correlation function of a fluid of hard spheres with diameter d_{WCA} and $u_{HS}(r; d_{WCA})$ is the corresponding potential. The above condition is based on the assumption that the long-wavelength part of the Fourier transforms of the pair correlation functions of both fluids, the reference fluid with the potential $u_0(r)$ of Eq. (8) and the HS fluid, with potential $u_{HS}(r; d_{WCA})$, will be equal, that is, $\hat{h}_0(k) \approx \hat{h}_{d_{WCA}}(k)$, which is accurately fulfilled at high densities [29]. Although the effective diameter d_{WCA} was defined within the context of the WCA perturbation theory, condition (10) is a reasonable approximation for any perturbation theory that uses a HS reference fluid, not only from a conceptual point of view, as seems clear from the preceding explanation, but also from mathematical considerations [31].

Closely related to the WCA is the Lado [30] proposal

$$\int \left[e^{-\beta u_0(r)} - e^{-\beta u_{HS}(r; d_L)} \right] \frac{\partial y_{HS}(r; d_L)}{\partial d_L} r^2 dr = 0, \tag{13}$$

which enforces thermodynamic consistency between the energy and virial routes to the equation of state.

In the WCA and Lado approximations the effective diameter is temperature- and density-dependent and is somewhat cumbersome to obtain. In Ref. [32] were reported expressions, fitted to the numerically calculated values, for the effective diameters in these two approximations.

3.2. Monte Carlo calculation of the perturbation terms in the HTE

In the *high-temperature expansion* (HTE), the Helmholtz free energy is expressed in the form

$$\frac{F}{Nk_BT} = \sum_{n=0}^\infty \frac{F_n}{Nk_BT} \frac{1}{T^{*n}}, \tag{14}$$

where $T^* = k_B T/\varepsilon$ is the reduced temperature and F_n is the nth perturbation term of the Helmholtz free energy. Other thermodynamic properties are readily obtained from the above expansion.

The zero-order term in expansion (14) is the Helmholtz free energy of the reference fluid. If the latter is the HS fluid, F_0 can be readily obtained from integration of the accurate Carnahan–Starling equation [33], with the result

$$\frac{F_0}{NK_BT} = \ln\left(\frac{\Lambda^3 \rho}{e}\right) + \frac{(4-3\eta)\eta}{(1-\eta)^2}, \tag{15}$$

where Λ is the thermal wavelength and $\eta = (\pi/6)\rho d^3$ is the packing fraction for hard spheres with diameter d at number density $\rho = N/V$.

The first-order term F_1 in the HTE (14) can be obtained accurately from the HS radial distribution function and higher-order terms can be obtained with quite good accuracy from the numerical solution of the so-called *coupling parameter series expansion* [34–37], based on a combination of perturbation theory with integral equation theory. Alternatively, several of the first terms in the series can be obtained from computer simulation, as done in the present work. The first three terms can be obtained from averages performed by computer simulations in the HS reference system from the expressions [3]

$$\frac{F_1}{Nk_BT} = \frac{1}{N}\sum_i \langle N_i\rangle_0 u_1^*(r_i), \tag{16}$$

$$\frac{F_2}{Nk_BT} = -\frac{1}{2N}\sum_{ij}\left\{\langle N_1 N_j\rangle_0 - \langle N_i\rangle_0\langle N_j\rangle_0\right\}u_1^*(r_i)u_1^*(r_j), \tag{17}$$

$$\frac{F_3}{Nk_BT} = -\frac{1}{6N}\sum_{ijk}\left\{\langle N_i N_j N_k\rangle_0 - 3\langle N_i N_j\rangle_0\langle N_k\rangle_0\right.$$

$$\left. +2\langle N_i\rangle_0\langle N_j\rangle_0\langle N_k\rangle_0\right\}u_1^*(r_i)u_1^*(r_j)u_1^*(r_k), \tag{18}$$

respectively, where N_i is the number of molecular distances in the interval r_i, r_{i+1}, with $\Delta r = r_{i+1} - r_i \ll \sigma$, $i = 1, 2, \ldots$, angular brackets mean averages, and subscript 0 means that the averages are performed in the HS reference system.

We have performed Monte Carlo NVT computer simulations to obtain the perturbation terms $F_1 - F_3$ of the LJ fluid with the d_{WCA} and d_L approximations for the HS effective diameter. For practical use, these data have been fitted to polynomials of the form

$$\frac{F_n}{NkT} = \sum_i \sum_j a_{nij}T^{*i}\rho^{*j}, \tag{19}$$

where $\rho^* = N\sigma_{LJ}^3/V$ is the reduced density of the Lennard-Jones fluid.

4. Results and discussion

Eq. (14), with Eqs. (15) and (19) constitute a third-order Monte Carlo based perturbation theory (MCPT). The perturbation terms F_n are different for the d_{WCA} and d_L effective diameters. However, with the σ_{LJ} and ε_{LJ} parameters determined in this work (see Table 2) we have found that the results obtained with d_L are much better, on the whole, than those obtained with d_{WCA}, and so the following analysis will restrict to the former and, for completeness, the corresponding parameters in Eq. (19) are listed in Table 4.

4.0.1. Argon
In Fig. 4 the liquid–vapor coexistence densities of Ar, obtained from the MCPT, are compared with the experimental data taken from the NIST compilation [38].

As we can see, the theory provides fairly good agreement with experimental data, although slightly overestimates the liquid densities at low temperatures, up to $\sim$ 4%, as well the critical temperature, by an amount of $\sim$ 2.5% for the latter.

Fig. 5 compares the MCPT results for the energy and the pressure of argon as a function of the density with the NIST compilation [38] at different supercritical temperatures and up to very high temperatures and pressures. In both cases, the agreement between theory and experiment is very good, although at high temperatures and densities the predicted values of the energy are slightly low and those for the pressure slightly high.

4.0.2. Krypton
For the predicted liquid–vapor coexistence of Kr similar conclusions as for Ar can be drawn, as seen in Fig. 6. Again the coexistence densities for the liquid phase are slightly overestimated at low temperatures, up to $\sim$ 3%, and the calculated critical temperature is $\sim$ 2.7% higher than the experimental one.

Concerning energy and pressure, Fig. 7 shows that both quantities are predicted with excellent accuracy.

Table 4

Parameters a_{nij} in Eq. (19) with the d_L approximation for the effective diameter.

| i	j				
		1	2	3	4	5
		n = 1				
0		−5.977843	−2.019346	−0.264093	0.711520	
1		0.827712	−2.337173	1.577166	−0.843582	
2		−0.284087	0.974040	−1.123063	0.662971	
		n = 2				
0		−1.543083	4.341932	−4.157844	1.315804	
1		0.342791	1.123952	−3.603604	2.208882	
2		−0.193636	−1.246914	3.353462	−1.962768	
3		0.042643	0.364380	−0.931332	0.536422	
		n = 3				
0		−0.568997	1.008044	0.316898	−1.324304	0.565868
1		0.472016	−0.563359	0.346115	−1.195348	0.937934
2		−0.369248	0.417766	−0.178282	0.674511	−0.516596
3		0.095133	−0.093651	−0.011436	−0.078979	0.078465
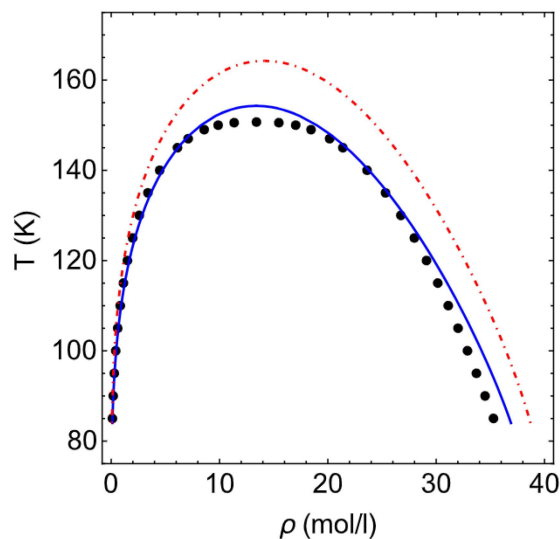
Fig. 4. Liquid–vapor coexistence for Ar. Points are the experimental data taken from the NIST compilation [38] and the continuous and dot-dashed curves are the present calculations from the MCPT with $\lambda = -0.77$ with and without the 3B contribution, respectively.

4.0.3. Xenon

The situation is quite different for Xe. As we can see in Fig. 8, the theory, with the values of σ_{LJ} and ε_{LJ} determined in this work from second virial coefficient data, considerably underestimates the coexistence liquid densities at all temperatures and slightly underestimates the vapor coexistence densities at temperatures close to the critical point, although the critical temperature itself is predicted quite accurately. The situation much improves if we use for the LJ potential parameters those obtained from solid state properties [20], although still near the critical point the liquid/vapor densities are slightly overpredicted/underpredicted, while the critical temperature is estimated with high accuracy.

The theoretical values for the energy of Xe, shown in Fig. 9, are in quite good agreement with experimental data, except at low temperatures and very high densities, for which the theory increasingly overestimates the magnitude of the energy with decreasing temperature. In this case both sets of potential parameters provide quite similar results, although slightly better those obtained from solid state properties. Instead, the theory strongly overestimates the pressures obtained from the potential parameters determined in this work, as is clearly seen in Fig. 9, at all temperatures and densities, whereas with the parameters obtained from solid state properties the predicted pressures are in quite good agreement with experiment.

It is somewhat surprising the fact that, within the context of the present theory, for Xe the LJ potential parameters determined from the lattice constant and the sublimation energy [20] provide better agreement with experiment for the thermodynamic properties of the fluid than those determined here from second virial coefficient data. However, we must
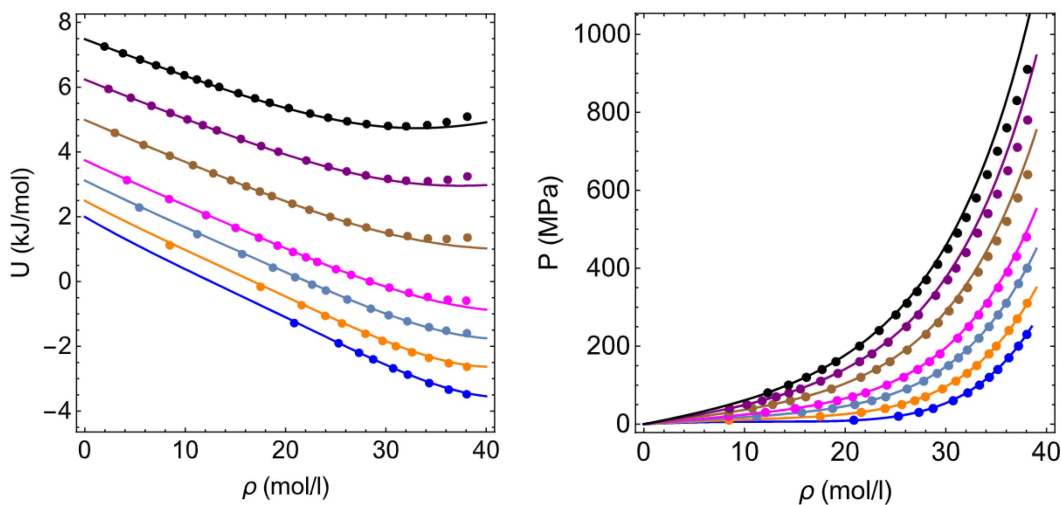
Fig. 5. Energy (left) and pressure (right) of Ar at T = 160, 200, 250, 300, 400, 500 and 600 K, respectively, from down up. Points are the experimental data from the NIST compilation [38] and the curves are the present calculations from the MCPT with λ given by Eq. (6).
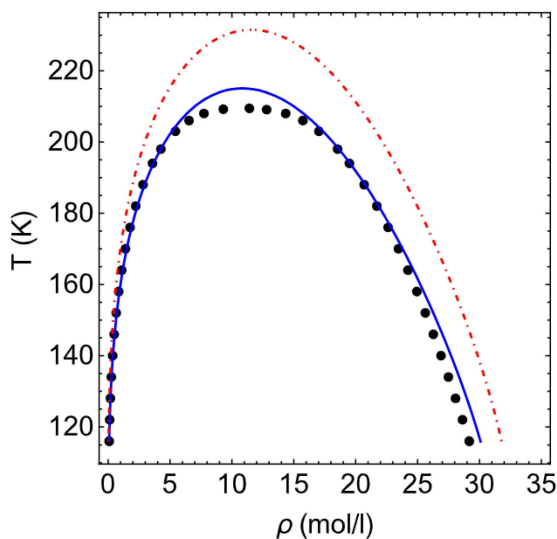

Fig. 6. Liquid–vapor coexistence for Kr. Points are the experimental data taken from the NIST compilation [38] and the continuous and dot-dashed curves are the present calculations from the MCPT with $\lambda = -0.77$ with and without the 3B contribution, respectively.

return to the comments previously made in Section 2 in relation with the potential parameters quoted in Table 2. There we noted that for Ar the LJ potential parameters determined from the two procedures are nearly equal and for Kr the distance parameters are also equal and the energy parameter are quite close to each other, and so the thermodynamic properties are accurately predicted by any of the two sets of parameters. In contrast, for Xe the potential parameters obtained in this work, and those reported in the literature, from second virial coefficient data, are quite different of those obtained from solid state properties. It is to be noted that the parameters obtained from the first of these procedures are subject to considerable uncertainty, whereas this seems not to be the case for those obtained from the second method. The fact is that the calculated thermodynamic properties are sensitive to the potential parameters. More specifically, the energy is particularly sensitive to the energy parameter ε and the pressure is strongly sensitive to the distance parameter σ.

The sensitivity of our theory to the potential parameters is its main weakness, although it cannot be attributed in advance to the theory itself but to the uncertainty in the values of the parameters. In any case, this sensitivity is shared in general with most other theories, unless the potential parameters are determined from the fitting of certain thermodynamic properties to experimental data.

On the opposite side, one of the main strengths of the present theory is its generality because, as already pointed out, it can be applied to any fluid whose two-body interactions are satisfactorily described by the Lennard-Jones potential, in
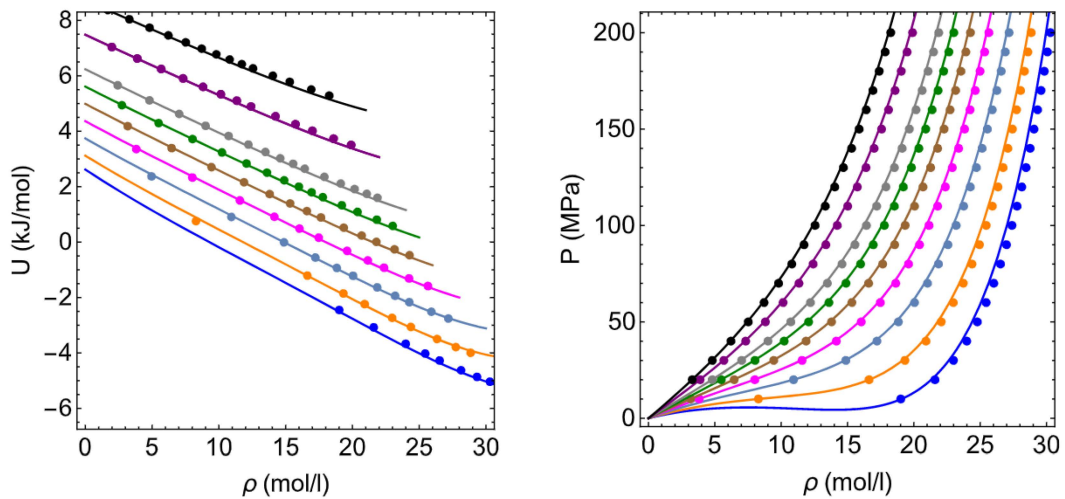
Fig. 7. Energy (left) and pressure (right) of Kr at $T = 210, 250, 300, 350, 400, 450, 500, 600$ and 700 K, respectively, from down up. Points are the experimental data from the NIST compilation [38] and the curves are the present calculations from the MCPT with λ given by Eq. (6).
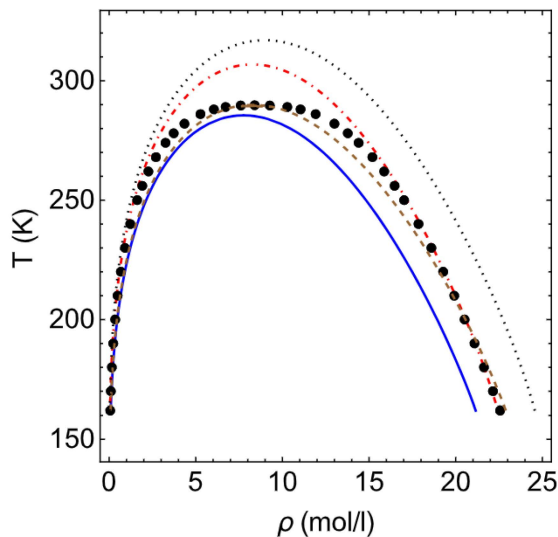

Fig. 8. Liquid–vapor coexistence for Xe. Points are the experimental data taken from the NIST compilation [38] and the curves are the present calculations with $\lambda = -0.77$. Continuous and dot-dashed curves correspond to $\sigma_{LJ} = 4.07$ Å, $\varepsilon_{LJ}/k = 223.6$ K with and without the 3B contribution, respectively. Dashed and dotted curves correspond to $\sigma_{LJ} = 3.96$ Å, $\varepsilon_{LJ}/k = 231.1$ K with and without the 3B contribution, respectively.

contrast with most other approximations proposed in the literature that are system dependent, as is the case of those reported in Refs. [4,5,8,10]. Another remarkable fact is that, although it was not expected in advance for a theory that does not account specifically for critical phenomena, our theory provides fairly good predictions for the coexistence curves.

On the other hand, the theory should not be used for reduced effective densities $\rho^* = \rho d^3 > 0.9$, because the simulations performed to obtain the perturbation terms F_n were carried out in the range $\rho^* = 0.1 - 0.9$.

One may wonder about the relative importance o using a perturbation theory of first, second, third, or even higher order. Of course, at strongly supercritical temperatures, a first-order perturbation theory would be enough accurate. The situation is different at temperatures close to the critical point or lower. For instance, the present theory with the three-body contribution overestimates the predicted critical temperatures for Ar by an amount of 9.7%, 4, 3%, and 2.5%, at first, second and third order, respectively, and similar results are obtained for Kr and Xe. From the relative magnitude of the first three terms it seems likely that considering still higher order terms will not improve significantly the results, apart from the fact that accurately calculating these terms by simulation would require a strong simulation effort.
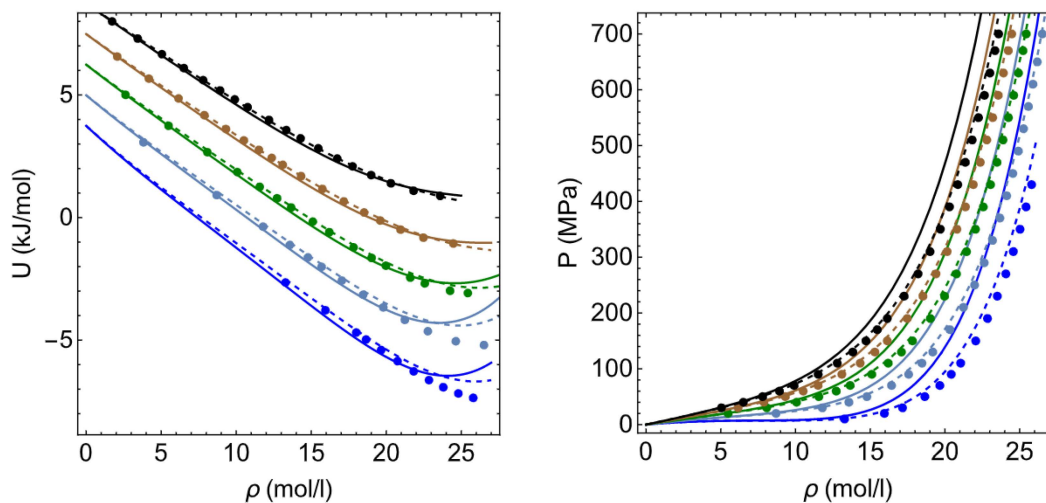
Fig. 9. Energy (left) and pressure (right) of Xe at $T = 300, 400, 500, 600$ and 700 K, respectively, from down up. Points are the experimental data taken from the NIST compilation [38]; the curves are the present calculations from the MCPT with λ given by Eq. (6), and with $\sigma_{LJ} = 4.07$ Å, $\varepsilon_{LJ}/k = 223.6$ (continuous), and $\sigma_{LJ} = 3.96$ Å, $\varepsilon_{LJ}/k = 231.1$ (dashed).

5. Concluding remarks

In the preceding sections we have developed a perturbation theory, within the framework of the high temperature expansion with the perturbation terms up to third order obtained by Monte Carlo simulation, with and effective two-body Lennard-Jones potential with the contribution of three-body interactions included following the procedures devised by Sadus et al. [13–16]. We have shown that the theory can provide accurate predictions for the coexistence densities and equilibrium properties of the heavy noble gases, provided that the LJ potential parameters are suitably chosen. In particular, the deviation in the predicted critical temperatures of Ar and Kr is less than 3% and still lower for Xe. The liquid coexistence densities of Ar and Kr at low temperatures are slightly overestimated, although by less than 3%, whereas the relative deviations in the predicted liquid and vapor coexistence densities of Xe near the critical point are greater, partially because these densities are relatively low. In any case, there is a strong improvement in the predicted coexistence curves by including the three-body contributions as compared with the situation where they are neglected. Surprisingly enough, we have found that the best results, on the whole, are obtained by using the LJ potential parameters obtained [20] from the lattice constant and sublimation energy of the solid, instead of those obtained from second virial coefficient data, as one might have expected.

The accuracy of the theory seems to be enough to be suitable for predictive and interpolation purposes, perhaps by using some optimization procedure to obtain the potential parameters, such as those used in Refs. [39,40]. For the latter purposes, generally resort is made to empirical correlations specific for each fluid. The advantage of our theory is that a single analytical expression can be applied to any fluid with pair interactions satisfactorily described by the Lennard-Jones potential, such as is the case of the noble gases considered here. Certainly, there are potential models more accurate for these substances, such as the BFW potential [17], but this has the disadvantage that they cannot be expressed in reduced units, so that the expression for the Helmholtz free energy, and any derived thermodynamic property, must be specific for each fluid.

CRediT authorship contribution statement

B.P. Akhouri: Formal analisis, Investigation. **J.R. Solana:** Supervision, Software, Writing – original draft.

Declaration of competing interest

The authors declare that they have no known competing financial interests or personal relationships that could have appeared to influence the work reported in this paper.

Data availability

The data have been included in the Supplemental Material

Appendix A. Supplementary data

Supplementary material related to this article can be found online at https://doi.org/10.1016/j.physa.2022.128280.

References

[1] J.R. Solana, Perturbation theories for the thermodynamic properties of fluids and solids, CRC Press, 2013.
[2] J.A. Barker, D. Henderson, Perturbation theory and equation of state for fluids: The square-well potential, J. Chem. Phys. 47 (1967) 2856–2861.
[3] J.A. Barker, D. Henderson, What is "Liquid"? Understanding the states of matter, Rev. Modern Phys. 48 (1976) 587–671.
[4] J.A. Barker, D. Henderson, W.R. Smith, Three-body forces in dense systems, Phys. Rev. Lett. 21 (1968) 134–136.
[5] S. Dridi, M.B. Amar, M. Abderraba, J.-P. Passarello, Development of a fully analytical equation of state using ab initio interaction potentials. Application to pure simple fluids: Noble gases Ne, Ar, Kr, and Xe, Fluid Phase Equilib. 562 (2022) 113563.
[6] Y. Tang, Y.-Z. Lin, Y.-G. Li, First-order mean spherical approximation for attractive, repulsive, and multi-Yukawa potentials, J. Chem. Phys. 122 (2005) 184505.
[7] I.A. McLure, J.E. Ramos, F. del Río, Accurate effective potentials and virial coefficients in real fluids. 1. Pure noble gases and their mixtures, J. Phys. Chem. B 103 (1999) 7019–7030.
[8] F. del Río, O. Guzmán, J.E. Ramos, B. Ibarra-Tandi, Effective intermolecular potentials in theoretical thermodynamics of pure substances and solutions, Fluid Phase Equilib. 259 (2007) 9–22.
[9] O. Guzmán, F. del Río, J.E. Ramos, Effective potential for three-body forces in fluids, Mol. Phys. 109 (6) (2011) 955–967.
[10] F. del Río, E. Díaz-Herrera, O. Guzmán, J.A. Moreno-Razo, J.E. Ramos, Analytical equation of state with three-body forces: Application to noble gases, J. Chem. Phys. 139 (2013) 184503.
[11] B.M. Axilrod, E. Teller, Interaction of the van der waals type between three atoms, J. Chem. Phys. 11 (1943) 299–300.
[12] H. Stenschke, Effective Axilrod-Teller interaction in van der Waals gases and liquids, J. Chem. Phys. 100 (1994) 4704–4705.
[13] G. Marcelli, R.J. Sadus, A link between the two-body and three-body interaction energies of fluids from molecular simulation, J. Chem. Phys. 112 (2000) 6382–6385.
[14] G. Marcelli, The role of three-body interactions on the equilibrium and non-equilibrium properties of fluids from molecular simulation. (Ph.D. thesis), Swinburne University of Technology, 2001.
[15] G. Marcelli, B.D. Todd, R.J. Sadus, On the relationship between two-body and three-body interactions from nonequilibrium molecular dynamics simulation, J. Chem. Phys. 115 (2001) 9410–9413.
[16] L. Wang, R.J. Sadus, Relationships between three-body and two-body interactions in fluids and solids, J. Chem. Phys. 125 (2006) 144509.
[17] J.A. Barker, R.A. Fisher, R.O. Watts, Liquid argon: Monte Carlo and molecular dynamics calculations, Mol. Phys. 21 (1971) 657–673.
[18] J.H. Dymond, E.B. Smith, The Virial Coefficients of Pure Gases and Mixtures. A Critical Compilation, Clarendon Press, Oxford, 1980.
[19] D.M. Heyes, G. Rickayzen, S. Pieprzyk, A.C. Brańka, The second virial coefficient and critical point behavior of the mie potential, J. Chem. Phys. 145 (2016) 084505.
[20] G. Horton, Ideal rare-gas crystals, Amer. J. Phys. 36 (1968) 93–119.
[21] P.J. Leonard, J.A. Barker, Dipole oscillator strengths and related quantities for inert gases, in: H. Eyring, D. Henderson (Eds.), in: Theoretical Chemistry: Advances and Perspectives, 1, Academic Press, London, 1975, pp. 117–136.
[22] E. Whalley, W.G. Schneider, Intermolecular potentials of argon, krypton, and xenon, J. Chem. Phys. 23 (1955) 1644–1650.
[23] R. Sadus, Two-body intermolecular potentials from second virial coefficient properties, J. Chem. Phys. 150 (2019) 024503.
[24] A. Beattie, R.J. Barriault, J.S. Brierley, The compressibility of gaseous krypton. II. The virial coefficients and potential parameters of krypton, J. Chem. Phys. 20 (1952) 1615–1618.
[25] A. Beattie, R.J. Barriault, J.S. Brierley, The compressibility of gaseous xenon. II. The virial coefficients and potential parameters of xenon, J. Chem. Phys. 19 (1951) 1222–1226.
[26] R. Bell, Multipolar expansion for the non-additive third-order interaction energy of three atoms, Phys. B: Atom. Mol. Phys. 3 (1970) 751–762.
[27] G. Marcelli, R.J. Sadus, Molecular simulation of the phase behavior of noble gases using accurate two-body and three-body intermolecular potentials, J. Chem. Phys. 111 (1999) 1533–1540.
[28] D. Chandler, J.D. Weeks, Equilibrium srtucture of simple liquids, Phys. Rev. Lett. 25 (1970) 149–152.
[29] J.D. Weeks, D. Chandler, H.C. Andersen, Role of repulsive forces in determining the equilibrium structure of simple liquids, J. Chem. Phys. 54 (1971) 5237–5247.
[30] F. Lado, Choosing the reference system for liquid state pertyurbation theory, Mol. Phys. 52 (1984) 871–876.
[31] T. van Western, J. Gross, A critical evaluation of perturbation theories by Monte Carlo simulation of the first four perturbation terms in a Helmholtz energy expansion for the Lennard-Jones fluid, Chem. Phys. 147 (2017) 014503.
[32] B.P. Akhouri, J.R. Solana, On the choice of the effective diameter in the high-temperature expansion for the Lennard–Jones fluid, Mol. Phys. 120 (2022) e2028918.
[33] N.F. Carnahan, K.E. Starling, Equation of state for nonattracting rigid spheres, J. Chem. Phys. 51 (1969) 635–636.
[34] S. Zhou, Thermodynamic perturbation theory in fluid statistical mechanics, Phys. Rev. E 74 (2006) 031119.
[35] S. Zhou, Improvement on macroscopic compressibility approximation and beyond, J. Chem. Phys. 125 (2006) 144518.
[36] A.S.V. Ramana, S.V.G. Menon, Coupling-parameter expansion in thermodynamic perturbation theory, Phys. Rev. E 87 (2013) 022101.
[37] A. Ramana, On equivalence of high temperature series expansion and coupling parameter series expansion in thermodynamic perturbation theory of fluids, J. Chem. Phys. 140 (2013) 154106.
[38] NIST Chemistry Webbook. http://dx.doi.org/10.18434/T4D303. [online].
[39] J. Vrabec, J. Stoll, H. Hasse, A set of molecular models for symmetric quadrupolar fluids, J. Phys. Chem. B 105 (2001) 12126–12133.
[40] G. Rutkai, M. Thol, R. Span, J. Vrabec, How well does the lennard-jones potential represent the thermodynamic properties of noble gases? Mol. Phys. 115 (2017) 1104–1121.